www.sciencemag.org/cgi/content/full/314/5804/1464/DC1

Supporting Online Material for

Microfluidic Digital PCR Enables Multigene Analysis of Individual Environmental Bacteria

Elizabeth A. Ottesen, Jong Wook Hong, Stephen R. Quake, Jared R. Leadbetter*

*To whom correspondence should be addressed. E-mail: jleadbetter@caltech.edu

Published 1 December 2006, *Science* **314**, 1464 (2006)
DOI: 10.1126/science.1131370

This PDF file includes:

MICROFLUIDIC DIGITAL PCR ENABLES MULTIGENE ANALYSIS OF INDIVIDUAL ENVIRONMENTAL BACTERIA

Supporting Online Materials

SUPPORTING TEXT: Design and validation of primers and probes for microfluidic digital PCR

Amplification of formyltetrahydrofolate synthetase genes from termite gut acetogens. Primers and probes were designed to specifically amplify FTHFS genes from "*Clone H Group*" acetogens, which comprised 43% of the *Zootermopsis* FTHFS clones inventoried by Salmassi and Leadbetter (*1*). These primers are distinct from those previously employed to amplify FTHFS genes from pure cultures and environmental samples (*2-5*). The newly designed primers and probes were tested for on-chip amplification and specificity using purified plasmid DNA (Fig. S1). The copy number as deduced from the number of positive chambers detected (adjusted based on a Poisson distribution of template) fell within 11-110% of the copy number calculated based on the concentration of double-stranded DNA in the template plasmid preparation. Freeze-thaw and template age may be one variable influencing observed amplification efficiencies; it has been recently reported that amplification efficiency can approach 99%(*6*). A small amount of amplification was detected from closely related clones (Fig. S1i), with a signal to background ratio less than half of that detected in positive clones. This low level of amplification from closely related species was also apparent in later experiments, as several FTHFS clones mapping to the "*Clone P Group*" were retrieved from on-chip reactions (see main text). No fluorescent signal was detected from amplification of distant relatives (clostridial and non-acetogenic FTHFS types, Fig. S1k). FTHFS copies were also detectable within DNA extracted from whole termite guts and from termite gut cell suspensions.

FTHFS simplex experiments used DyNAzyme II polymerase (Finnzymes) at 0.2 units per µl and 1x TaqMan Universal PCR Master Mix (Applied Biosystems) for real-time PCR. Due to the high concentration of detergent in the enzyme storage buffer, only 0.05% Tween-20 (Sigma) was added. All other experiments described used the iTaq system described in the main body of the paper, as this enzyme was found to perform well on the chip at lower concentrations, and had hot-start capabilities to ensure that the enzyme was inactive during the chip loading process.

Design of "*all-bacterial*" 16S rRNA primers and probes. Primers and probes for amplification of bacterial 16S rRNA were also employed. Bacterial 16S rRNA genes detected in on-chip amplification from termite gut community DNA preparation amounted to 1.4×10^5 copies per ng (1 copy every 6.7 MB DNA), which was 5.9-fold higher than the copy number deduced by real-time PCR using *Treponema primitia* ZAS-2 genomic DNA as a standard. Background amplification has been reported in a number of general bacterial 16S real-time assays, and is commonly attributed to DNA fragments present in commercial enzyme preparations (*7*). In on-chip experiments with the final primer set, negative controls never exceeded 1.2% positive chambers (1.9 copies per µl).

Specific detection of termite cluster treponemes through use of a spirochete-specific reverse primer with the broad-range forward primer and probe. A 16S rRNA gene reverse primer was designed that matched 41 out of 60 termite gut spirochetes with sequence data covering the primer site. Of the known 16S rRNA sequences that did not match the primer, three were associated with the "*termite gut treponeme*" ribotype cluster (*8*). The remaining mismatches were with sequences affiliated with "*treponeme subgroup 1*" (*9*), which respresents less than 1% of spirochetal 16S clones amplified from *Z. nevadensis* using conventional methods and other spirochete-specific primers (*unpublished data*, primers from Lilburn, Schmidt, and Breznak (*8*)). Our new primers were tested for specificity and efficiency in simplex and multiplex reactions with FTHFS primers/probes using conventional and real-time PCR methods. In on-chip PCR reactions using purified PCR products as template they detected 11% of the expected copy number.

MATERIALS AND METHODS

Termite Maintenance. *Zootermopsis nevadensis* specimens were collected from fallen Jeffrey (*Pinus jeffreyi*) and Ponderosa Pine (*Pinus ponderosa*) at Mt. Pinos in the Los

Padres National Forest and at the Chilao Flats Campground in the Angeles National Forest. Colonies were maintained in the laboratory on Ponderosa at 23 C and at a constant humidity of 96%, achieved via incubation over saturated solutions of KH_2PO_4 within 10-gallon aquaria (*10*).

PCR on Microfluidic Chips. Microfluidic devices were purchased from Fluidigm Corporation (www.fluidigm.com/didIFC.htm). On-chip multiplex PCR reactions contained 0.05 units · μl-1 iTaq DNA polymerase (BioRad), iTaq PCR buffer, 200 μM each dNTP, 1.5 mM $MgCl_2$, and 0.1% Tween-20. In almost all PCR reactions, primers and probes were used at 400 nM; all bacterial 16S primers were used at 600 nM in on-chip reactions. Primers and probes were purchased from Integrated DNA Tecnologies and had the following sequences: FTHFS forward, 5′-GAATCACGCGAAGACTGGTTC-3′; reverse, 5′-TTGAGTTACAACCGTGTGCGAT-3′; probe, 5′-CAAGGCGCAATGGCAGCCCT-3′ (FAM and Black Hole Quencher 1 labelled), all bacterial rRNA 357 forward 5′-CTCCTACGGGAGGCAGCAG-3′ (modified from (*11*)), 1492 reverse 5′-TACGGYTACCTTGTTACGACTT-3′ (modified from (*12*)); 1389 reverse probe 5′-CTTGTACACACCGCCCGTC-3′ (described in (*13*), labelled with CY5 and Iowa Black quencher). Termite gut spirochete-specific SSU rRNA amplification was achieved using the 1389R probe and 357F primer with a spirochete-specific 1409R primer (sequence 5′-GGGTACCTCCAACTCGGATGGTG-3′).

Zootermopsis hindguts were extracted from worker larvae, suspended in sterile TE (10 mM Tris-HCl, 1 mM EDTA, pH 8), and disrupted via repeated aspiration using a 1 ml Eppendorf pipettor. Suspensions were allowed to stand briefly to sediment large particles, then diluted to working concentrations in TE and mixed 1 to 10 with the PCR reaction mixture (above) for immediate loading onto microfluidic chips.

Chips were loaded using air pressure. 200 μl gel loading tips were filled with sample and connected to air lines at 12-15 PSI (pounds per square inch) pressure. Control channels were loaded with 35% PEG (polyethylene glycol) 3350 (ca. 50 μl, in gross excess). The 12 sample channels were loaded with 15 μl of PCR reaction (again, in excess). After loading, sample lines were allowed to re-equilibrate to atmospheric pressure. Control valves were closed by the application of 25 PSI air pressure to control lines.

Cycling was carried out on flat-block thermocyclers (MJ Research). Microscope immersion oil (Cargille, Type FF) was applied between the chip and thermocycling block, and the cycling program was as follows: 98°C 30s, 97°C 30s, 95°C 2min, [56°C 30s, 58°C 30s, 60°C 30s, 98°C 15s] x 40 cycles, 60°C for 10 min.

Reaction results were evaluated by fluorescent signal strength as measured using an ArrayWoRx scanner (Applied Precision). Spot intensities were located and retrieved using either ArrayWoRx software or the ScanAlyze program (version 2.50, Michael Eisen). Cutoff values for positive amplification were calculated for each sample panel independently. Chambers in the bottom 25% of the intensity range were assumed to contain no amplification, and positive chambers were defined as chambers whose spot intensity was more than 10 standard deviations above the mean of points in this range for the FTHFS probe. The 16S rRNA gene probe gave a more variable signal, so the threshold for this channel was set at 5 standard deviations above the mean.

Sample Retrieval and Analysis. Single cell PCR products were retrieved from amplification-positive chambers. Chips were peeled from the backing slide, and pressure was removed from control channels (most valves remained fused despite relief of external pressure). Target chambers were located using a dissecting microscope, and the tip of a 30 gauge syringe needle was inserted into each chamber through the bottom surface of the chip. Needles were then swirled briefly in 10 μl of TE to desorb the PCR product.

Retrieval efficiency was checked by real time PCR using the same primers as above in BioRad SYBR Green PCR Master Mix. Reactions were carried out using the Chromo4 system (BioRad), and temperature program 95°C 3min, (95°C 15s, 60°C 1min30s) x 40 cycles. FTHFS concentration standards contained a 1.2 kb section of 'ZA-gut Clone U' type FTHFS gene sequence (*1*). Termite community DNA was used as a standard for all bacterial 16S rRNA gene PCR, and *T. primitia* ZAS-2 genomic DNA for spirochete-specific reactions. Samples that contained 104 or more gene copies were deemed successful retrievals.

Retrieved PCR products were amplified for cloning and/or sequencing using EXPAND high fidelity polymerase (Roche), Fail-Safe PCR PreMix D (Epicentre), and primers and cycling conditions as above. PCR products were purified using the Qiagen PCR purification kit, and sequenced using the FTHFS PCR primers and 16S rRNA gene internal primers 1100R and 533F (5′-AGGGTTGCGCTCGTTG-3′ and 5′-GTGCCAGCMGCCGCGGTAA-3′, respectively; modified from ref. (*12*)). Some samples contained a mixture of 16S rRNA sequences. These sequences were cloned using the TOPO TA cloning kit for sequencing (Invitrogen). Eight colonies from each cloning reaction were picked and used as template for high-fidelity PCR as described above. 10 μl of each reaction was digested at 37°C for 2 hr with 3 units HinPI1 from New England Biolabs and analyzed by agarose gel electrophoresis. A representative of each RFLP (restriction fragment length polymorphism) type was prepared for sequencing as described above, using recommended T3 and T7 primers. All sequencing reactions were carried out by the California Institute of Technology DNA Sequencing Facility.

Sequences were assembled and edited using the Lasergene software package (DNASTAR, Inc). Phylogenetic analysis and alignment of 16S rRNA gene sequences was carried out using the ARB software package (*14*). FTHFS sequences were translated into protein, and aligned using GenomatixSuite software (Genomatix). Nucleic acid sequences were aligned according to the protein alignment. All 16S rRNA gene sequences were screened using chimera identification programs Bellerophon (*15*) and Pintail (*16*). Three chimeric sequences were identified and eliminated from further analysis.

Real-Time PCR Standards and DNA Template Preparation. Plasmid templates were purified from *E. coli* strains from the library of Salmassi and Leadbetter using the Qiaprep Spin Miniprep Kit (Qiagen). Termite gut community DNA was extracted from the pooled gut contents of five termites. Guts were disrupted using the protocol laid out in Salmassi and Leadbetter (*1*), with the substitution of TE (10 mM Tris-HCl, 1 mM EDTA, pH 8) for the phosphate buffer described in that paper. After bead-beating and phenol extraction, DNA was purified from the aqueous phase using the Qiagen DNeasy Tissue kit, with the protocol described for extraction of DNA from crude lysates (DNeasy Tissue Handbook, July 2003 version). Template concentrations were measured using the Hoefer DyNAQuant 200 fluorometer and DNA quantification system (amersham pharmacia biotech) using reagents and procedures directed in the manual (DQ200-IM, Rev C1, 5-98). Termite gut cell suspensions were prepared as described in the main body of the paper.

SUPPORTING REFERENCES

1. T. M. Salmassi, J. R. Leadbetter, *Microbiol.* **149**, 2529 (Sep, 2003).
2. M. Pester, A. Brune, *Environ Microbiol* **8**, 1261 (Jul, 2006).
3. A. B. Leaphart, C. R. Lovell, *Appl. Environ. Microbiol.* **67**, 1392 (Mar, 2001).
4. A. B. Leaphart, M. J. Friez, C. R. Lovell, *Appl Environ Microbiol* **69**, 693 (Jan, 2003).
5. C. R. Lovell, A. B. Leaphart, *Methods Enzymol* **397**, 454 (2005).
6. L. Warren, D. Bryder, I. L. Weissman, S. R. Quake, *Proc Natl Acad Sci U S A* (Nov 10, 2006).
7. C. E. Corless *et al.*, *J. Clin. Microbiol.* **38**, 1747 (May, 2000).
8. T. G. Lilburn, T. M. Schmidt, J. A. Breznak, *Environ. Microbiol.* **1**, 331 (Aug, 1999).
9. B. J. Paster *et al.*, *J Bacteriol* **173**, 6101 (Oct, 1991).
10. P. W. Winston, Bates, Donald H., *Ecology* **41**, 232 (January, 1960, 1960).
11. M. A. Nadkarni, F. E. Martin, N. A. Jacques, N. Hunter, *Microbiol.* **148**, 257 (Jan, 2002).
12. D. J. Lane, in *Nucleic Acid Techniques in Bacterial Systematics* M. G. E. Stackebrandt, Ed. (Wiley, New York, 1991) pp. 115-175.
13. M. T. Suzuki, L. T. Taylor, E. F. DeLong, *Appl. Environ. Microbiol.* **66**, 4605 (Nov, 2000).
14. W. Ludwig *et al.*, *Nucl. Acids Res.* **32**, 1363 (2004).
15. T. Huber, G. Faulkner, P. Hugenholtz, *Bioinformatics* **20**, 2317 (Sep 22, 2004).
16. K. E. Ashelford, N. A. Chuzhanova, J. C. Fry, A. J. Jones, A. J. Weightman, *Appl. Environ. Microbiol.* **71**, 7724 (Dec, 2005).
17. J. R. Leadbetter, T. M. Schmidt, J. R. Graber, J. A. Breznak, *Science* **283**, 686 (Jan 29, 1999).
18. T. G. Lilburn *et al.*, *Science* **292**, 2495 (Jun 29, 2001).
19. M. D. Kane, J. A. Breznak, *Arch. Microbiol.* **156**, 91 (1991).
20. W. G. Weisburg *et al.*, *J Bacteriol* **171**, 6455 (Dec, 1989).
21. M. D. Kane, A. Brauman, J. A. Breznak, *Arch. Microbiol.* **156**, 99 (1991).
22. A. Loy, W. Beisker, H. Meier, *Appl. Environ. Microbiol.* **71**, 3624 (Jul, 2005).
23. S. Noda, M. Ohkuma, A. Yamada, Y. Hongoh, T. Kudo, *Appl. Environ. Microbiol.* **69**, 625 (Jan, 2003).
24. H. Yang, D. Schmitt-Wagner, U. Stingl, A. Brune, *Environ. Microbiol.* **7**, 916 (Jul, 2005).
25. Y. Hongoh, M. Ohkuma, T. Kudo, *FEMS Microbiol. Ecol.* **44**, 231 (2003).
26. I. GrechMora *et al.*, *Int. J. Syst. Bacteriol.* **46**, 512 (Apr, 1996).
27. C. Wyss, B. K. Choi, P. Schüpbach, B. Guggenheim, U. B. Göbel, *Int. J. Syst. Bacteriol.* **47**, 842 (Jul, 1997).
28. C. Wyss, B. K. Choi, P. Schüpbach, B. Guggenheim, U. B. Göbel, *Int. J. Syst. Bacteriol.* **46**, 745 (Jul, 1996).

Table S1: Sequences Used for Phylogenetic Analysis

Source/Sequence Type	Designation	Gene	Accession	Reference	Figures
T. primitia ZAS-1	ZAS-1	16S	AF093251	(*17*)	Fig. 2, Sup. Fig. 2
T. primitia ZAS-2	ZAS-2	16S	AF093252	(*17*)	Fig. 2, Sup. Fig. 2
T. azotonutricium ZAS-9	ZAS-9	16S	AF320287	(*18*)	Fig. 2, Sup. Fig. 2
T. primitia ZAS-1	ZAS-1a	FTHFS	AY162313	(*1*)	Fig. 2
T. primitia ZAS-2	ZAS-2	FTHFS	AY162315	(*1*)	Fig. 2
T. azotonutricium ZAS-9	ZAS-9	FTHFS	AY162316	(*1*)	Fig. 2
Z. angusticollis Gut Clone	A	FTHFS	AY162294	(*1*)	Fig 2, Sup. Fig. 1
Z. angusticollis Gut Clone	C	FTHFS	AY162295	(*1*)	Sup. Fig. 1
Z. angusticollis Gut Clone	E	FTHFS	AY162296	(*1*)	Sup. Fig. 1
Z. angusticollis Gut Clone	E2	FTHFS	AY162297	(*1*)	Sup. Fig. 1
Z. angusticollis Gut Clone	F	FTHFS	AY162298	(*1*)	Sup. Fig. 1
Z. angusticollis Gut Clone	F2	FTHFS	AY162299	(*1*)	Sup. Fig. 1
Z. angusticollis Gut Clone	G	FTHFS	AY162300	(*1*)	Sup. Fig. 1
Z. angusticollis Gut Clone	G2	FTHFS	AY162301	(*1*)	Fig 2, Sup. Fig. 1
Z. angusticollis Gut Clone	H	FTHFS	AY162302	(*1*)	Fig 2, Sup. Fig. 1
Z. angusticollis Gut Clone	I	FTHFS	AY162303	(*1*)	Fig 2, Sup. Fig. 1
Z. angusticollis Gut Clone	L	FTHFS	AY162304	(*1*)	Sup. Fig. 1
Z. angusticollis Gut Clone	M	FTHFS	AY162305	(*1*)	Sup. Fig. 1
Z. angusticollis Gut Clone	N	FTHFS	AY162306	(*1*)	Sup. Fig. 1
Z. angusticollis Gut Clone	P	FTHFS	AY162307	(*1*)	Fig 2, Sup. Fig. 1
Z. angusticollis Gut Clone	R	FTHFS	AY162308	(*1*)	Fig 2, Sup. Fig. 1
Z. angusticollis Gut Clone	T	FTHFS	AY162309	(*1*)	Sup. Fig. 1
Z. angusticollis Gut Clone	U	FTHFS	AY162310	(*1*)	Sup. Fig. 1
Z. angusticollis Gut Clone	Y	FTHFS	AY162311	(*1*)	Sup. Fig. 1
Z. angusticollis Gut Clone	Z	FTHFS	AY162312	(*1*)	Sup. Fig. 1
Z. nevadensis Genomovar	ZEG 10.1	FTHFS	DQ420342	This study	Fig. 2
Z. nevadensis Genomovar	ZEG 10.2	FTHFS	DQ420343	This study	Fig. 2
Z. nevadensis Genomovar	ZEG 10.3	FTHFS	DQ420344	This study	Fig. 2
Z. nevadensis Genomovar	ZEG 10.4	FTHFS	DQ420345	This study	Fig. 2
Z. nevadensis Genomovar	ZEG 11.1	FTHFS	DQ420346	This study	Fig. 2
Z. nevadensis Genomovar	ZEG 11.2	FTHFS	DQ420347	This study	Fig. 2
Z. nevadensis Genomovar	ZEG 11.3	FTHFS	DQ420348	This study	Fig. 2
Z. nevadensis Genomovar	ZEG 11.4	FTHFS	DQ420349	This study	Fig. 2
Z. nevadensis Genomovar	ZEG 11.5	FTHFS	DQ420350	This study	Sup. Fig. 2
Z. nevadensis Genomovar	ZEG 11.6	FTHFS	DQ420351	This study	Sup. Fig. 2
Z. nevadensis Genomovar	ZEG 11.7	FTHFS	DQ420352	This study	Sup. Fig. 2
Z. nevadensis Genomovar	ZEG 12.1	FTHFS	DQ420353	This study	Fig. 2
Z. nevadensis Genomovar	ZEG 12.2	FTHFS	DQ420354	This study	Fig. 2
Z. nevadensis Genomovar	ZEG 12.3	FTHFS	DQ420355	This study	Fig. 2
Z. nevadensis Genomovar	ZEG 12.4	FTHFS	DQ420356	This study	Fig. 2
Z. nevadensis Genomovar	ZEG 12.5	FTHFS	DQ420357	This study	Sup. Fig. 2
Z. nevadensis Genomovar	ZEG 13.1	FTHFS	DQ420358	This study	Fig. 2
Z. nevadensis Genomovar	ZEG 10.1	16S	DQ420325	This study	Fig. 2
Z. nevadensis Genomovar	ZEG 10.2	16S	DQ420326	This study	Fig. 2
Z. nevadensis Genomovar	ZEG 10.3	16S	DQ420327	This study	Fig. 2
Z. nevadensis Genomovar	ZEG 10.4	16S	DQ420328	This study	Fig. 2
Z. nevadensis Genomovar	ZEG 11.1	16S	DQ420329	This study	Fig. 2
Z. nevadensis Genomovar	ZEG 11.2	16S	DQ420330	This study	Fig. 2
Z. nevadensis Genomovar	ZEG 11.3	16S	DQ420331	This study	Fig. 2
Z. nevadensis Genomovar	ZEG 11.4	16S	DQ420332	This study	Fig. 2
Z. nevadensis Genomovar	ZEG 11.5	16S	DQ420333	This study	Sup. Fig. 2
Z. nevadensis Genomovar	ZEG 11.6	16S	DQ420334	This study	Sup. Fig. 2
Z. nevadensis Genomovar	ZEG 11.7	16S	DQ420335	This study	Sup. Fig. 2

Z. nevadensis Genomovar	ZEG 12.1	16S	DQ420336	This study	Fig. 2
Z. nevadensis Genomovar	ZEG 12.2	16S	DQ420337	This study	Fig. 2
Z. nevadensis Genomovar	ZEG 12.3	16S	DQ420338	This study	Fig. 2
Z. nevadensis Genomovar	ZEG 12.4	16S	DQ420339	This study	Fig. 2
Z. nevadensis Genomovar	ZEG 12.5	16S	DQ420340	This study	Sup. Fig. 2
Z. nevadensis Genomovar	ZEG 13.1	16S	DQ420341	This study	Fig. 2
Z. nevadensis Gut Clone	Zn-FG1	16S	DQ420259	This study	Sup. Fig. 3
Z. nevadensis Gut Clone	Zn-FG2A	16S	DQ420263	This study	Sup. Fig. 3
Z. nevadensis Gut Clone	Zn-FG2B	16S	DQ420264	This study	Sup. Fig. 3
Z. nevadensis Gut Clone	Zn-FG3	16S	DQ420275	This study	Sup. Fig. 3
Z. nevadensis Gut Clone	Zn-FG4	16S	DQ420273	This study	Sup. Fig. 3
Z. nevadensis Gut Clone	Zn-FG5A	16S	DQ420269	This study	Sup. Fig. 3
Z. nevadensis Gut Clone	Zn-FG5C	16S	DQ420270	This study	Sup. Fig. 3
Z. nevadensis Gut Clone	Zn-FG6	16S	DQ420271	This study	Sup. Fig. 3
Z. nevadensis Gut Clone	Zn-FG7A	16S	DQ420266	This study	Fig. 2, Sup. Fig. 2
Z. nevadensis Gut Clone	Zn-FG7B	16S	DQ420262	This study	Fig. 2, Sup. Fig. 2
Z. nevadensis Gut Clone	Zn-FG8A	16S	DQ420284	This study	Sup. Fig. 3
Z. nevadensis Gut Clone	Zn-FG9	16S	DQ420317	This study	Sup. Fig. 3
Z. nevadensis Gut Clone	Zn-FG10	16S	DQ420319	This study	Sup. Fig. 3
Z. nevadensis Gut Clone	Zn-FG11A	16S	DQ420272	This study	Sup. Fig. 3
Z. nevadensis Gut Clone	Zn-FG11B	16S	DQ420258	This study	Sup. Fig. 3
Z. nevadensis Gut Clone	Zn-FG12	16S	DQ420261	This study	Sup. Fig. 3
Z. nevadensis Gut Clone	Zn-FG13A	16S	DQ420286	This study	Sup. Fig. 3
Z. nevadensis Gut Clone	Zn-FG13B	16S	DQ420287	This study	Sup. Fig. 3
Z. nevadensis Gut Clone	Zn-FG14	16S	DQ420257	This study	Sup. Fig. 3
Z. nevadensis Gut Clone	Zn-FG15A	16S	DQ420277	This study	Sup. Fig. 3
Z. nevadensis Gut Clone	Zn-FG15B	16S	DQ420278	This study	Sup. Fig. 3
Z. nevadensis Gut Clone	Zn-FG15C	16S	DQ420279	This study	Fig. 2, Sup. Fig. 2
Z. nevadensis Gut Clone	Zn-FG16A	16S	DQ420280	This study	Sup. Fig. 3
Z. nevadensis Gut Clone	Zn-FG16B	16S	DQ420281	This study	Sup. Fig. 3
Z. nevadensis Gut Clone	Zn-FG17A	16S	DQ420282	This study	Sup. Fig. 3
Z. nevadensis Gut Clone	Zn-FG17B	16S	DQ420283	This study	Sup. Fig. 3
Z. nevadensis Gut Clone	Zn-FG18A	16S	DQ420255	This study	Sup. Fig. 3
Z. nevadensis Gut Clone	Zn-FG18B	16S	DQ420276	This study	Sup. Fig. 3
Z. nevadensis Gut Clone	Zn-G1	16S	DQ420256	This study	Sup. Fig. 3
Z. nevadensis Gut Clone	Zn-G2	16S	DQ420254	This study	Fig. 2, Sup. Fig. 2
Z. nevadensis Gut Clone	Zn-G3	16S	DQ420265	This study	Sup. Fig. 3
Z. nevadensis Gut Clone	Zn-G4A	16S	DQ420310	This study	Sup. Fig. 3
Z. nevadensis Gut Clone	Zn-G4B	16S	DQ420311	This study	Sup. Fig. 3
Z. nevadensis Gut Clone	Zn-G4C	16S	DQ420312	This study	Sup. Fig. 3
Z. nevadensis Gut Clone	Zn-G5A	16S	DQ420313	This study	Sup. Fig. 3
Z. nevadensis Gut Clone	Zn-G5B	16S	DQ420314	This study	Sup. Fig. 3
Z. nevadensis Gut Clone	Zn-G6	16S	DQ420260	This study	Sup. Fig. 3
Z. nevadensis Gut Clone	Zn-G7	16S	DQ420268	This study	Sup. Fig. 3
Z. nevadensis Gut Clone	Zn-G8	16S	DQ420267	This study	Sup. Fig. 3
Z. nevadensis Gut Clone	Zn-G9	16S	DQ420315	This study	Sup. Fig. 3
Z. nevadensis Gut Clone	Zn-G10	16S	DQ420285	This study	Sup. Fig. 3
Z. nevadensis Gut Clone	Zn-G11	16S	DQ420274	This study	Sup. Fig. 3
Z. nevadensis Gut Clone	Zn-G12A	16S	DQ420316	This study	Sup. Fig. 3
Z. nevadensis Gut Clone	Zn-G12B	16S	DQ420324	This study	Sup. Fig. 3
Z. nevadensis Gut Clone	Zn-G13	16S	DQ420298	This study	Sup. Fig. 2
Z. nevadensis Gut Clone	Zn-G14	16S	DQ420299	This study	Sup. Fig. 2
Z. nevadensis Gut Clone	Zn-G15A	16S	DQ420320	This study	Sup. Fig. 3
Z. nevadensis Gut Clone	Zn-G15B	16S	DQ420321	This study	Sup. Fig. 3
Z. nevadensis Gut Clone	Zn-G15C	16S	DQ420322	This study	Sup. Fig. 3
Z. nevadensis Gut Clone	Zn-G16	16S	DQ420300	This study	Sup. Fig. 3

Z. nevadensis Gut Clone	Zn-G17	16S	DQ420301	This study	Sup. Fig. 3
Z. nevadensis Gut Clone	Zn-G18	16S	DQ420302	This study	Sup. Fig. 3
Z. nevadensis Gut Clone	Zn-G19	16S	DQ420303	This study	Sup. Fig. 3
Z. nevadensis Gut Clone	Zn-G20	16S	DQ420323	This study	Sup. Fig. 3
Z. nevadensis Gut Clone	Zn-FS1	16S	DQ420288	This study	Sup. Fig. 2
Z. nevadensis Gut Clone	Zn-FS2	16S	DQ420289	This study	Sup. Fig. 2
Z. nevadensis Gut Clone	Zn-S1A	16S	DQ420307	This study	Sup. Fig. 2
Z. nevadensis Gut Clone	Zn-S2	16S	DQ420295	This study	Sup. Fig. 2
Z. nevadensis Gut Clone	Zn-S3	16S	DQ420308	This study	Sup. Fig. 2
Z. nevadensis Gut Clone	Zn-S4A	16S	DQ420309	This study	Sup. Fig. 2
Z. nevadensis Gut Clone	Zn-S5	16S	DQ420296	This study	Sup. Fig. 2
Z. nevadensis Gut Clone	Zn-S6	16S	DQ420297	This study	Sup. Fig. 2
Z. nevadensis Gut Clone	Zn-S7A	16S	DQ420304	This study	Sup. Fig. 2
Z. nevadensis Gut Clone	Zn-S7B	16S	DQ420305	This study	Sup. Fig. 2
Z. nevadensis Gut Clone	Zn-S8	16S	DQ420290	This study	Sup. Fig. 2
Z. nevadensis Gut Clone	Zn-S9	16S	DQ420291	This study	Sup. Fig. 2
Z. nevadensis Gut Clone	Zn-S10	16S	DQ420292	This study	Sup. Fig. 2
Z. nevadensis Gut Clone	Zn-S11A	16S	DQ420306	This study	Sup. Fig. 2
Z. nevadensis Gut Clone	Zn-S12	16S	DQ420293	This study	Sup. Fig. 2
Z. nevadensis Gut Clone	Zn-S13	16S	DQ420294	This study	Sup. Fig. 2
Acetonema longum	APO-1	16S	M61919	(*19*)	Sup. Fig. 3
Acholeplasma laidlawii	JA1	16S	M23932	(*20*)	Sup. Fig. 3
Clostridium mayombei	SFC-5	16S	M62421	(*21*)	Sup. Fig. 3
Comamonadaceae Clone	C-6	16S	AF523013	(*22*)	Sup. Fig. 3
N. koshunensis symbiont	Nk-S93	16S	AB084970	(*23*)	Sup. Fig. 2
R. flavipes Gut Clone	RFS88	16S	AF068344	(*8*)	Sup. Fig. 2
R. santonensis Gut Clone	RsaHf236	16S	AY571482	(*24*)	Sup. Fig. 2
R. santonensis Gut Clone	RsaHf303	16S	AY571478	(*24*)	Sup. Fig. 2
R. speratus Gut Clone	Rs-B05	16S	AB088896	(*25*)	Sup. Fig. 2
R. speratus Gut Clone	Rs-B10	16S	AB088880	(*25*)	Sup. Fig. 2
R. speratus Gut Clone	Rs-B29	16S	AB088891	(*25*)	Sup. Fig. 2
R. speratus Gut Clone	Rs-D17	16S	AB089048	(*25*)	Sup. Fig. 3
R. speratus Gut Clone	Rs-D39	16S	AB089089	(*25*)	Sup. Fig. 3
R. speratus Gut Clone	Rs-D40	16S	AB088874	(*25*)	Sup. Fig. 2
R. speratus Gut Clone	Rs-D46	16S	AB088865	(*25*)	Sup. Fig. 2
R. speratus Gut Clone	Rs-E47	16S	AB088921	(*25*)	Sup. Fig. 3
R. speratus Gut Clone	Rs-F14	16S	AB088939	(*25*)	Sup. Fig. 3
R. speratus Gut Clone	Rs-F63	16S	AB088934	(*25*)	Sup. Fig. 3
R. speratus Gut Clone	Rs-E64	16S	AB088888	(*25*)	Fig. 2
R. speratus Gut Clone	Rs-K70	16S	AB089106	(*25*)	Sup. Fig. 3
R. speratus Gut Clone	Rs-M74	16S	AB089115	(*25*)	Sup. Fig. 3
R. speratus Gut Clone	Rs-P59	16S	AB088914	(*25*)	Sup. Fig. 2
R. speratus Gut Clone	Rs-Q39	16S	AB089075	(*25*)	Sup. Fig. 3
Sporomusa termitida	JSN-2	16S	M61920	(*19*)	Sup. Fig. 3
Termitobacter aceticus	SYR	16S	Z49863	(*26*)	Sup. Fig. 3
TM7 phylum Env. Clone	BU080	16S	AF385568		Sup. Fig. 3
Treponema amylovorum	HA2P	16S	Y09959	(*27*)	Sup. Fig. 2
Treponema denticola	II:11:33520	16S	M71236	(*9*)	Sup. Fig. 2
Treponema maltophilum	patient BR	16S	X87140	(*28*)	Sup. Fig. 2
Treponema pallidum	Nichols	16S	M88726	(*9*)	Sup. Fig. 2
Treponema phagedenis	K5	16S	M57739	(*9*)	Sup. Fig. 2

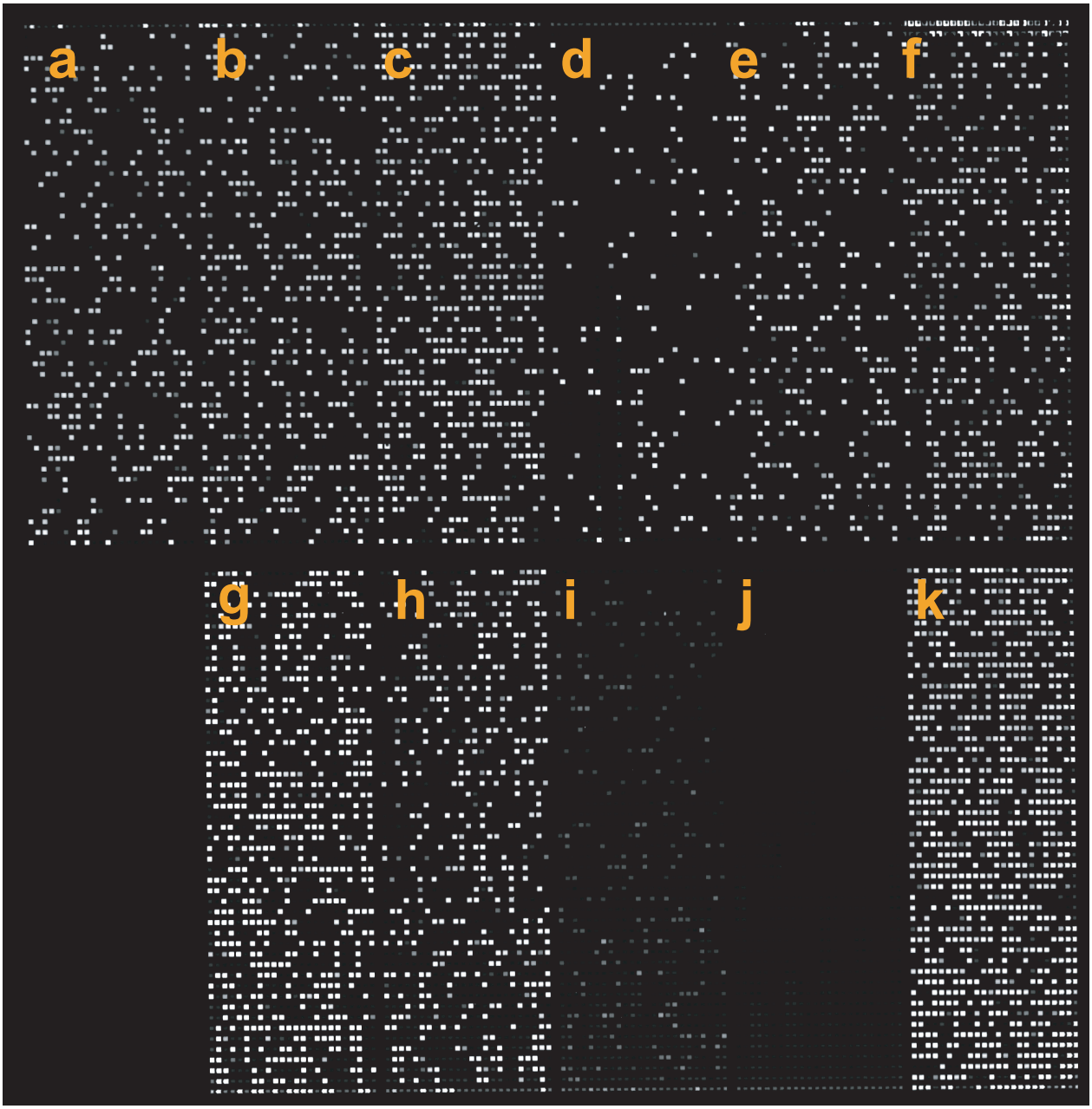

Figure S1: FTHFS primer specificity and demonstration of single copy sensitivity. A single microfluidic chip on which the FTHFS primers and probe were tested against purified plasmid templates. Panels **a** though **h** and **k** each show amplification from one of nine different Clone H Group FTHFS genotypes (each cloned into a plasmid), each at equal dsDNA concentrations. Panel **i** contains six pooled non-H type FTHFS genotypes that cluster within the termite treponeme FTHFS cluster (see *Salmassi & Leadbetter 2003*). Panel **j** contains four pooled FTHFS genotypes that that do not cluster phylogenetically with termite treponemes. All clones (and each clone within pooled templates) were added at DNA concentrations equivalent to ~200 copies per µl (one molecule per reaction chamber). Specific clone types and observed copy number are as follows: a.) Clone E2, 62 cp/µl; b.) Clone F2, 79 cp/µl; c.) Clone G2,121cp/µl; d.) Clone H, 22 cp/µl; e.) Clone I, 55 cp/µl; f.) Clone L, 91 cp/µl; g.) Clone U, 130 cp/µl; h.) Clone R, 82 cp/µl; I.) pooled, non target Clones G, P, Z, C, N, and A, 11 cp/µl; j.) pooled, non-target Clones F, T, Y, E, 0 copies detected; and k.) Clone M, 222 cp/µl. To allow cross-comparison of sample panels, a single threshold for positive amplification was calculated for the entire chip; this value was set to 5 standard deviations above the mean of chambers in the lowest 25% of the intensity range.

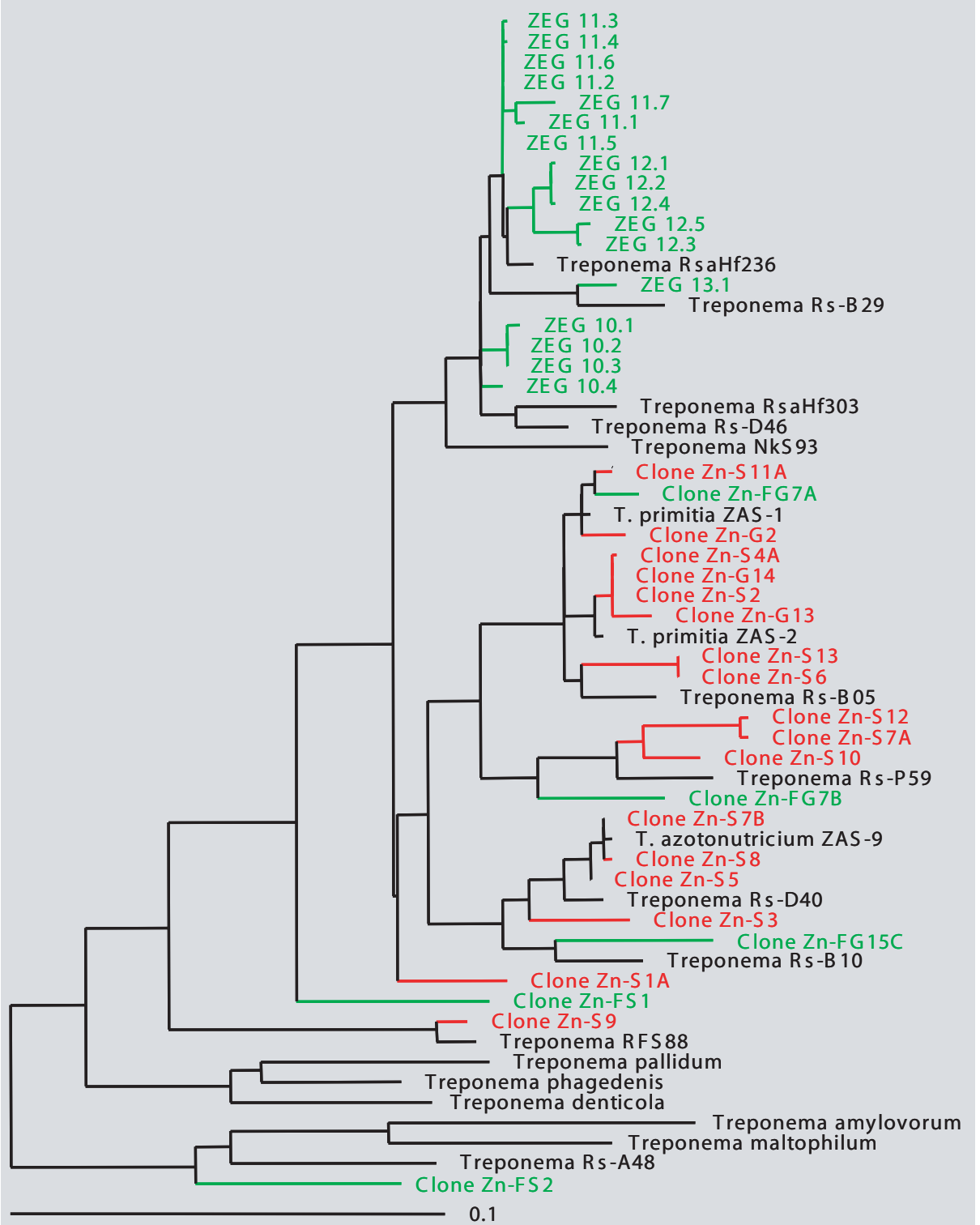

Figure S2: Phylogenetic Analysis of Termite Treponemal 16S rRNA sequences retrieved from microfluidic chips. rDNA sequences recovered from chambers in which only 16S rRNA genes were amplified are marked in red; they were assigned a Zn-G moniker when "*all bacterial*" primers were employed and a Zn-S moniker when spirochete-specific primers were employed. 16S rRNA gene sequences co-recovered with FTHFS sequences are marked in green; those that fell outside the ZEG cluster were assigned a Zn-FG or Zn-FS moniker according to the 16S rRNA gene primer set employed. ZEG genomovars 11.5, 11.6, 11.7, and 12.5 were identified in experiments using spirochete-specific rRNA primers. Tree was calculated using Phylip distance methods and 630 unambigous, aligned residues. Scale bar represents 0.1 changes per alignment position.

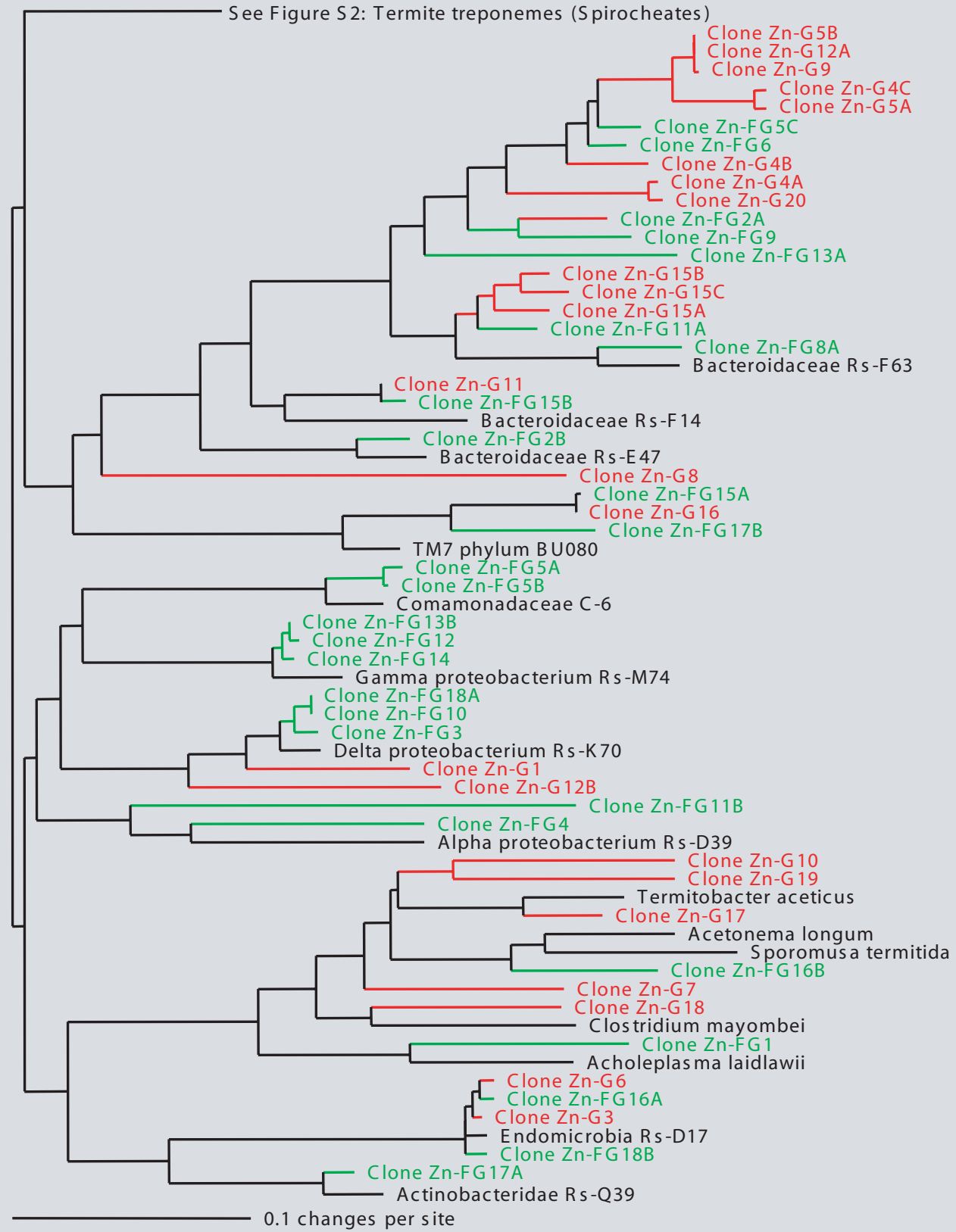

Figure S3: Phylogenetic Analysis of 16S rRNA sequences retrieved from microfluidic chips and close relatives. Sequence naming and color coding as described in Fig. S2. Tree was calculated using Phylip distance methods and 630 unambiguous, unaligned residues. Scale bar represents 0.1 changes per alignment position.